




Modelling and Structural Analysis of Tram Railway Vehicle Body with Finite Element Method

Willy Artha Wirawan¹ , Febry Pandu Wijaya², Dadang Sanjaya Atmaja¹, Fadli Rozaq¹, Aji Satria Bagaskara¹, and F. X. Prakosa Pamungkas¹

¹ Indonesian Railway Polytechnic, Tirta Raya Street, Manguharjo, 63161 Madiun, Indonesia
willy@pengajar.ppi.ac.id

² PT. Industri Kereta Api (INKA), Jl. Yos Sudarso No.71, Madiun Lor, Kec. Manguharjo, Kota Madiun, Jawa Timur 63122, Indonesia

Abstract. This study aims to model and analyze the design structure of the Tram car body using the finite element method. The help of software will compute a calculation to display a visual form of an estimate of the actual condition of a tram mover design. The simulation was carried out based on 5 cases of loading by the Regulation of the Minister of Transportation of the Republic of Indonesia No. 175 of 2015, which regulates the load that was applied according to car body testing and standardization. The output of this research was the maximum vertical deflection, von-misses stress, and the value of the safety factor. This simulation found that the maximum stress occurred at the end center sill of 148.16 MPa due to compression loading and the maximum vertical deflection value of 4.4058 mm on the roof due to vertical full load loading overall safety factor value from this Tram car body simulation was 1.6536. This value was still considered safe because it was still below the allowable stress required by standardization, which is 75% of 245 MPa (SS400 material permit stress) or 183.75 MPa.

Keywords: Carbody · finite element method · von-misses stress · deflection · safety factor

1 Introduction

Train as a means of human mobility is one of the most effective modes of transportation. Tram is rail-based transportation that has evolved from the evolution of the regular rail network into an urban-based passenger transportation service. Initially, the tram was pulled by horsepower. Then with the development of the industrial revolution, steam power began to be used, and eventually, electric or diesel power was now used. Tram is generally dense urban area transportation as an alternative in tackling congestion. Trams have advantages such as better elevation angles and turning radius when compared to other types of trains and have lower construction and operating costs. Tram can also be used as a tourism potential because of the uniqueness in its operation and has a difference from busways in general.

The fundamental difference between trains and trams is that trains are coarse-meshed, which means they have high speed, large capacity, independent infrastructure, and separate tracks from the road. In contrast, trams are fine-meshed, which means the infrastructure is semi-independent, or the rail tracks are integrated with the highway to operate simultaneously with other vehicles on the road.

The use of trams has now been developed in various cities and leading tourist areas such as the TMII (Taman Mini Indonesia Indah) area. Tram Mover was designed with a capacity of 8 passengers with an automatic control system. Tram Mover has the main construction of a car body and bogie. The car body tram construction consists of a roof, side walls, and an underframe consisting of a middle frame and a bolster. The side walls of the Tram Mover tend to be dominated by the glass with the aim that passengers can enjoy the view from the tour.

The car body of trains generally protects passengers and goods on the train. The body of the train is supported by a bogie which supports and protects the load caused by people and objects. The design of the car body must also have an aerodynamic appearance and have a high level of security against collisions during an accident so that this structure can prevent severe damage that occurs and also results in minimizing injuries or fatalities to passengers. The car body has a function as a support for the load on the passengers and the interior of the train, as well as to keep the train always in a severe condition, which means there is no material failure during operation (safe).

With the need for a structural safety level on the car body, it is important to conduct a design test on a product that will be manufactured. In this study, we presented modeling and analysis of the car body design on tram trains using ANSYS Workbench software. The main objective of this study was to determine the stress and amount of displacement by examining the car body strength of the sampled vehicle under the required loading and operating conditions. The car body design was based on the Tram Mover train reference that PT produced. Industri Kereta Api (INKA).

2 Research Method

The research method was quasi-experimental by conducting design simulations using FEM (finite element method) software. The output values generated from this simulation will be validated based on data from the tram mover design obtained from PT. Industri Kereta Api (INKA).

The loading conditions in the standard “EN 12663-1 - Rail Applications - Structural Properties of Railway Vehicle Bodies” were used to reference the mass of passengers in the vehicle. According to this standard, the mass of each passenger is 70 kg. In addition, the driver’s mass is accepted as 80 kg as a standard requirement.

3 Tram Design and Modelling

This Tram car body engineering drawing was designed and modeled using Autodesk Inventor software. This modeling was done by drawing the main parts of the car body, and the assembly process was carried out with a 3D model. The car body had dimensions of 5500 mm long × 2400 mm wide × 3000 mm high, designed with a passenger capacity of 8 people and an operating speed of 30 km/h Fig. 1.

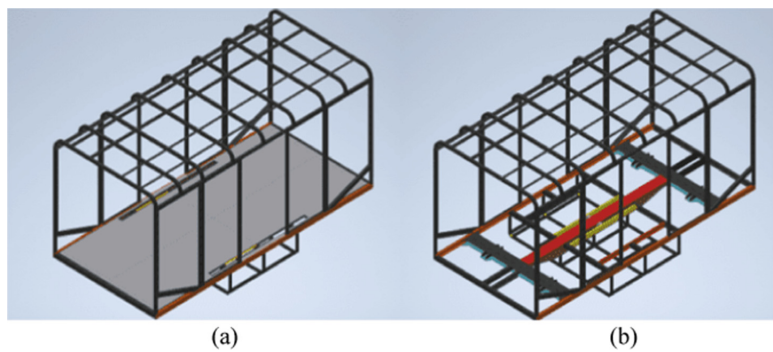


Fig. 1. Tram Mover (a) Carbody Design (b) Carbody Model

Table 1. Technical Specifications and tram load

	Specification	Mass (kg)	Actual Load (N) ($F = m \times g$)	E×ceptional Load (N) ($F = 1,3 \times m \times g$)
Passenger Capacity	8 Orang	560	5493,6	7141,68
Carbody	$550 \times 240 \times 300$ (cm)	820	8044,2	10457,64
AC Unit	8000 kcal/h	160	1569,6	2040,48
Battery	200 kWh	200	1962	2550,6
Bogie	Axle Width 1610 mm	464	4551,84	5917,392
Motor	7,5 Kilo Watt of Power	146	1432,26	1861,938
Total		1530	15009,3	19512,09

4 Material

The required materials were based on the Regulation of the Minister of Transportation: PM 175 of 2015, where the base frame was designed with welded assembled steel construction made of carbon steel or other materials. That has high strength and stiffness against loading without permanent deformation and was equipped with impact-resistant construction. The material specified in the construction of this underframe was Structural Steel SS400 (JIS G3101) for all main constructions in the form of plates and C profiles of the Tram car body underframe.

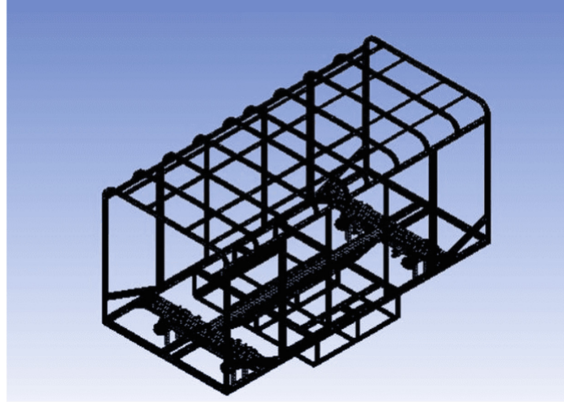


Fig. 2. Meshing on Tram Mover Carbody Design

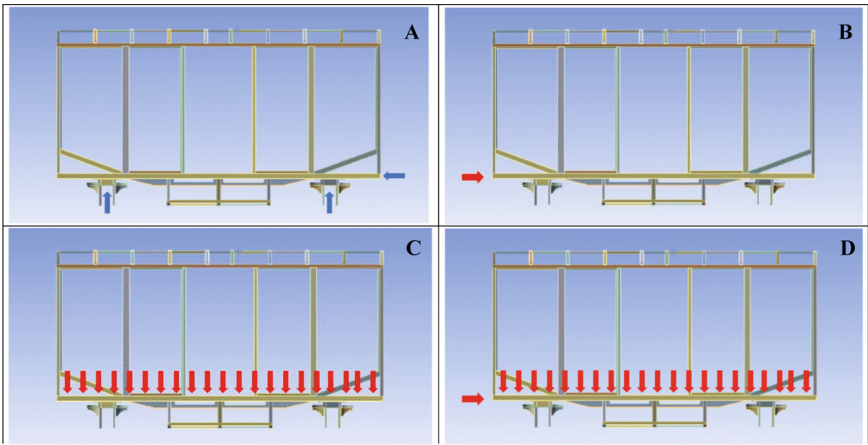


Fig. 3. (a) Illustration of Boundary Condition (b) Compression Load (c) Vertical Load (d) Combination Load

5 Meshing

The mesh used in this simulation was 50 mm in size and produced 539,792 nodes and 198,112 elements. This site was considered quite thorough for this car body modeling. The type of mesh formed was a hybrid, with the shape of the quadrilateral and triangular mesh used in this simulation Fig. 2.

6 Determining Boundary Conditions and Load

The boundary condition will be defined by providing a constraint. The constraint used in this simulation was displacement. This displacement will be given a value of 0 to the

Table 2. Mechanical Properties

Elastic Modulus	Poisson Ratio	Density	Yield Strength	Ultimate Strength
$2,1 \times 10^5$ (Mpa)	0,3	7850 (Kg/m ³)	245 (Mpa)	400 (Mpa)

X (longitudinal), Y (vertical), and Z (lateral) axis so that this condition can limit the motion of the object to be simulated Fig. 3.

Static load was carried out according to the standards required in the Regulation of the Minister of Transportation No. 175 of 2015. The main loading on the car body model was applied to the surface of the upper underframe and the bottom of the roof as a vertical load consisting of two subcases, namely vertical tare load $P_v = 1.3 \times (820 \text{ kg} + (0 \text{ kg})) = 1066 \text{ kg}$ (Loading on the car body added with loading on the roof). The second subcase vertical full load $P_v = 1.3 \times (1066 \text{ kg} + (8 \text{ people} \times 70 \text{ kg})) = 2113.8 \text{ kg}$ (Loading on the car body plus loading on the roof and full passengers) and at the end center sill as a compression load of 200 kN.

Table 3. Comparison of Simulation Results

No.	Load Case	Deflection (mm)	Stress (MPa) on Own Simulation	Stress (MPa) on PT INKA's Simulation	Location of maximum Stress	Material Type	Description
1	Compression Load	0,25765	148,16	140,24	<i>Side Sill</i>	SS 400	$\sigma_{max} < \text{allowed } \sigma$
2	<i>Vertical Tare Load</i>	4,2758	51,704	50,05	<i>Side Roof</i>	SS 400	$\sigma_{max} < \text{allowed } \sigma$
3	Compression Load and <i>Vertical Tare Load</i>	4,1241	146,85	146,44	<i>End Sill</i>	SS 400	$\sigma_{max} < \text{allowed } \sigma$
4	<i>Vertical Full Load</i>	4,4058	53,745	52,09	<i>Side Roof</i>	SS 400	$\sigma_{max} < \text{allowed } \sigma$
5	Compression Load and <i>Vertical Full Load</i>	4,2261	147,17	148,55	<i>End Sill</i>	SS 400	$\sigma_{max} < \text{allowed } \sigma$

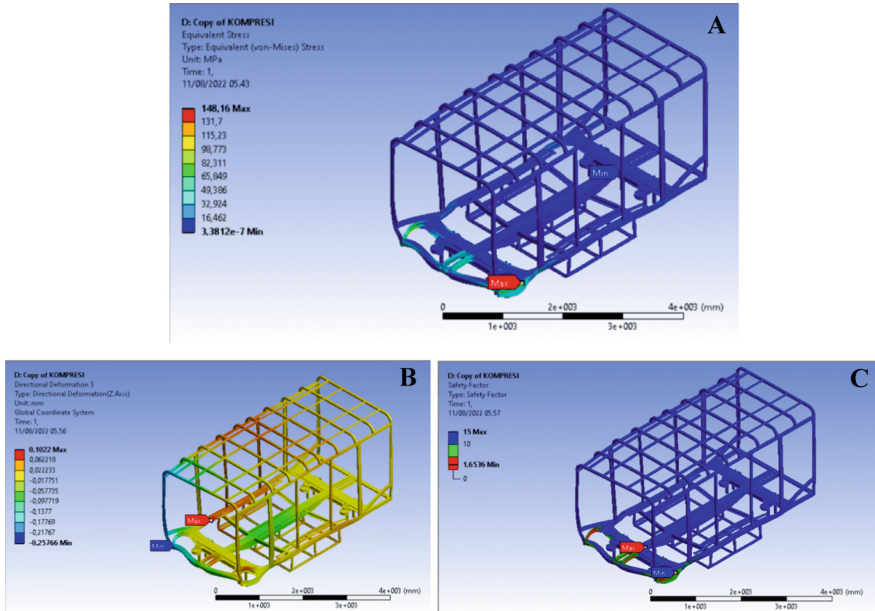


Fig. 4. Compression Load (a) Von-Mises Stress (b) maximum Vertical Deflection (c) Safety factor

7 Research Results

The simulation results obtained from the structural simulations carried out were in the form of the prevailing stress distribution and the maximum vertical deflection on each node. The voltage taken in this simulation was von-mises as the failure theory used was the theory of maximum energy distortion Table 2 and Table 3. The value that came out as the output in this simulation will be used as a reference for analyzing the structural strength of the car body. By the Minister of Transportation PM No. 175 of 2015, the maximum allowable stress is 75% of the Yield Strength Material used, which is 75% of 245 MPa, which is 183.75 for SS400 material (JIS G3101) Fig. 4.

7.1 Case of Compression Load

From the simulation carried out, it was obtained that the largest stress value was 148.16 MPa which occurred in the side sill due to compression loading of 200 kN in the longitudinal direction of the X axis. It was known that the maximum vertical deflection occurred on the Z axis of 0.25765 mm and occurred at the side sill due to compression loading with the longitudinal direction of the X axis. The smallest safety factor value was 1.6536 and was still within safe limits by standardization.

7.2 Case of Vertical Loading

Vertical loading was carried out in two subcases: vertical tare load and full vertical load. The following are the results of the vertical loading simulation Fig. 5.

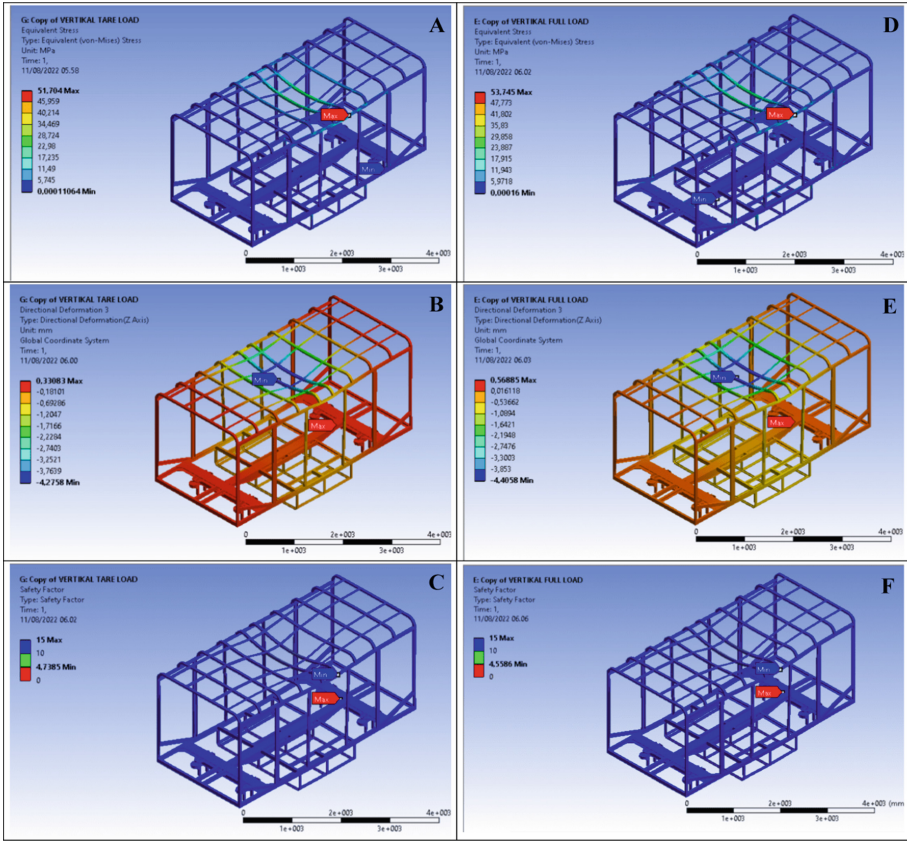


Fig. 5. (a) Von-Misses Stress on Vertical Tare Load (b) maximum Vertical Deflection Vertical Tare Load (c) Safety factor on Vertical Tare Load (d) Von-Misses Stress on Vertical Full Load (e) maximum Vertical Deflection on Vertical Full Load (f) Safety factor on Vertical Full Load

From the simulation, it was found that the maximum stress that occurred due to the case of vertical tare load loading was 51.704 MPa on the side roof. It was known that the maximum vertical deflection occurred on the Z axis of 4.2758 mm and occurred on the roof due to the loading of their conditioning system, while the smallest safety factor value was 4.7385. In the case of vertical loading, the full load was 53.745 MPa on the side roof. It was known that the maximum vertical deflection occurred on the Z axis of 4.4058 mm on the roof section and the smallest safety factor value was 4.5586. The simulation results show that under conditions of vertical tare load and full vertical load, they are still within safe limits according to standardization.

7.3 Combined Loading

There were two sub-cases of combined loading carried out by simulation: compression loading with vertical tare load and compression loading with the full vertical load. The following are the results of the combined loading simulation carried out

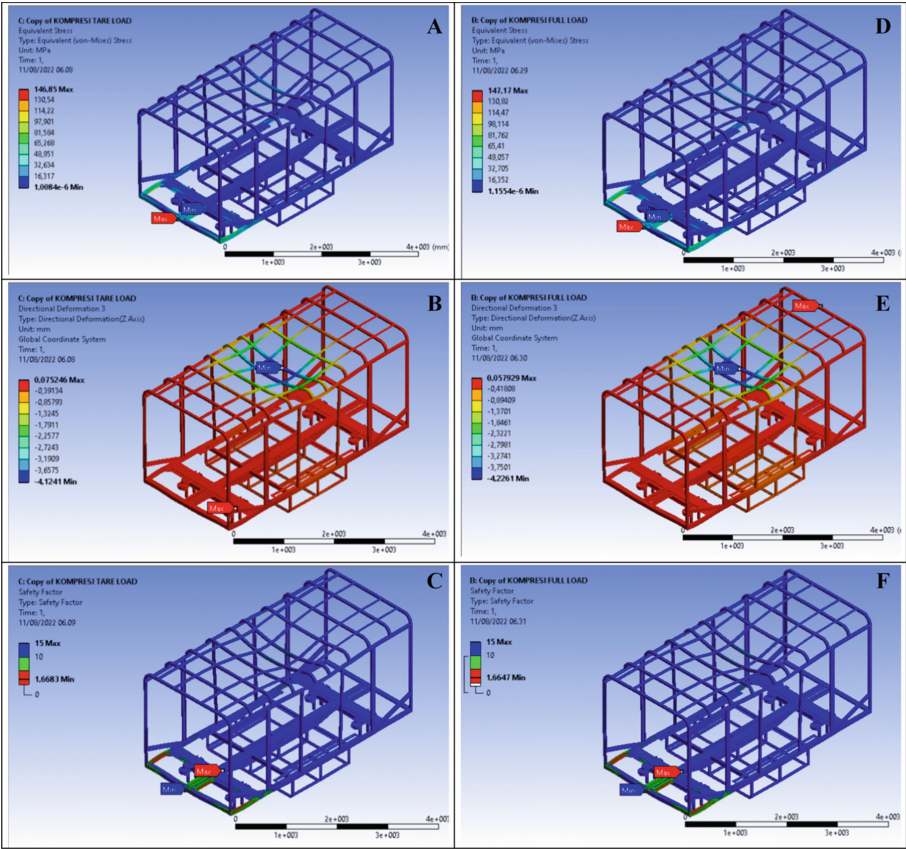


Fig. 6. Combination Load (a) Von-Misses Stress on Combination of Compression and Vertical Tare Load (b) Vertical Deflection on Combination of Compression and Vertical Tare Load (c) Safety factor Combination of Compression and Vertical Tare Load (d) Von-Misses Stress on Combination of Compression and Vertical Full Load (e) Vertical Deflection on Combination of Compression and Vertical Full Load (f) Safety factor on Combination of Compression and Vertical Full Load

Figure 6 shows that the maximum stress that occurred due to the combined loading case of compression and vertical tare load was 146.85 MPa at the end sill, while the maximum vertical deflection was 4.1241 mm on the -Z axis. The smallest safety factor value was 1.6684 mm. The maximum stress that occurred due to combined compression loading and vertical tare load was 147.17. The maximum vertical deflection was 4.2261 mm on the Z axis, and the smallest safety factor value was 1.6647 mm; thus, it was still within the safe limit according to the standard.

In Table 1, the difference in the error value between the two voltage results that occur in each test can be seen. The largest error value occurred in the first loading variation, namely compression loading, with an error value of 9.46%. The data obtained from the simulation results are valid because the deviation and error values are still below <10%.

8 Conclusions

In the simulation, it was found that the equivalent maximum von-mises stress occurred on the compression loading of 148.16 MPa on the side sill with a percentage of the SS400 material elongation stress of 60.47% from 245 MPa. These results indicated that it was still declared safe because the percentage value was still below 75% by the standardization of the Minister of Transportation's PM No. 175 of 2015. The simulations that were carried out showed that the maximum vertical deflection value occurred on the full load vertical loading subcase with a value of 4.4058 mm occurring on the roof due to vertical loading of the air conditioning system. The safety factor figure from the car body tram simulation was 1.6536 and was still declared safe by the standardization of EN-12663–1:2010.

References

1. European Standard. (2010). Railway Applications - Structural Requirements of Railway Vehicle Bodies - Part 1: Locomotives and passenger Rolling stock (and Alternative Method for Freight Wagons) Applications. European Committee For Standardization.
2. F. Rozaq, W. Artha Wirawan, A. Zulkarnaen, Jamaluddin, and H. Boedi Wahjono, "The Influence of Temperature and Lubrication Variation on the Dimension Change in Ring Compression Test Using Ansys Software," J. Phys. Conf. Ser., vol. 1273, no. 1, 2019, <https://doi.org/10.1088/1742-6596/1273/1/012080>.
3. Menteri Perhubungan Republik Indonesia. (2015). Peraturan Menteri Perhubungan Republik Indonesia No 175 Tahun 2015 tentang Standar Spesifikasi Teknis Kereta Kecepatan Normal dengan Penggerak Sendiri.
4. M. E. Ari and İ. Esen, "Design of a Metro Train and Structural Analysis of the Metro Vehicle Body by Finite Element Method", Demiryolu Mühendisliği, no. 15, pp. 30-45, 2022, <https://doi.org/10.47072/demiryolu.1018663>
5. S. Widi Astuti, W. Artha Wirawan, A. Zulkarnain, and D. Tri Istiantara, "Comparison of Energy Absorption and Pattern of Deformation Material Crash Box of Three Segments with Bilinear and Johnson Cook Approach," J. Phys. Conf. Ser., vol. 1273, no. 1, 2019, <https://doi.org/10.1088/1742-6596/1273/1/012078>.
6. W. Artha Wirawan, A. Zulkarnain, H. Boedi Wahjono, Jamaluddin, and A. Tyas Damayanti, "The Effect of Material Exposure Variations on Energy Absorption Capability and pattern of Deformation Material of Crash Box of Three Segments," J. Phys. Conf. Ser., vol. 1273, no. 1, 2019, <https://doi.org/10.1088/1742-6596/1273/1/012081>.

Open Access This chapter is licensed under the terms of the Creative Commons Attribution-NonCommercial 4.0 International License (<http://creativecommons.org/licenses/by-nc/4.0/>), which permits any noncommercial use, sharing, adaptation, distribution and reproduction in any medium or format, as long as you give appropriate credit to the original author(s) and the source, provide a link to the Creative Commons license and indicate if changes were made.

The images or other third party material in this chapter are included in the chapter's Creative Commons license, unless indicated otherwise in a credit line to the material. If material is not included in the chapter's Creative Commons license and your intended use is not permitted by statutory regulation or exceeds the permitted use, you will need to obtain permission directly from the copyright holder.

